Magnetohydrodynamic Modeling of Plasma Channels for Acceleration and Beam Transport

Nathan Cook*+, Stephen Coleman*, Abdourahmane Diaw*, Jonathan Edelen*
Edward Hansen**, Petros Tzeferacos**

+ncook@radiasoft.net

* RadiaSoft LLC, Boulder, CO
**University of Rochester, Rochester, NY

2022 Advanced Accelerator Concepts Workshop

November 7, 2022

This material is based upon work supported by the U.S. Department of Energy, Office of Science, Office of High Energy Physics under Award Number(s) DE-SC0018719.

Structured plasmas present unique opportunities for accelerators

Plasma channels act as waveguides for intense lasers

- Ohmic heating generates slowly evolving parabolic profile which may be matched to a Gaussian laser spot

$$n_p(r) = n_0 + \Delta n \frac{r^2}{W_0^2}$$

- Matching preserves laser spot and mode structure over many Rayleigh ranges

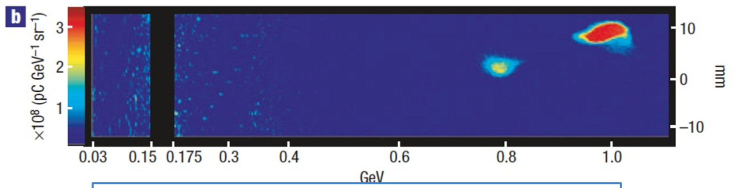

Nat. Phys. **2**, 696-699 (2006)

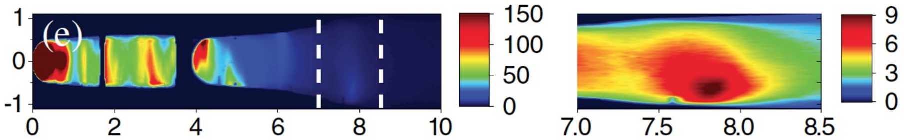

Phys. Rev. Lett. **122**, 084801 (2019)

Flexible beam transport of high energy beams, and high divergence beams

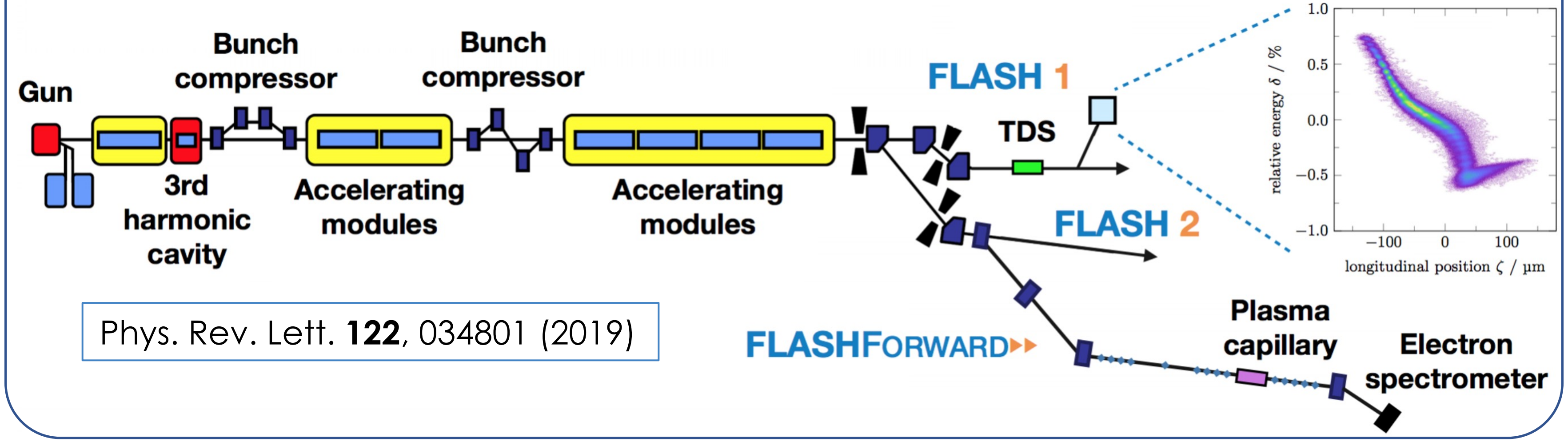

Phys. Rev. Lett. **122**, 034801 (2019)

Plasma ramps mitigate emittance growth

- Adiabatic ramping of plasma density enables beam matching at entrance, exit of plasma
- Buffer gases introduce unique design challenges

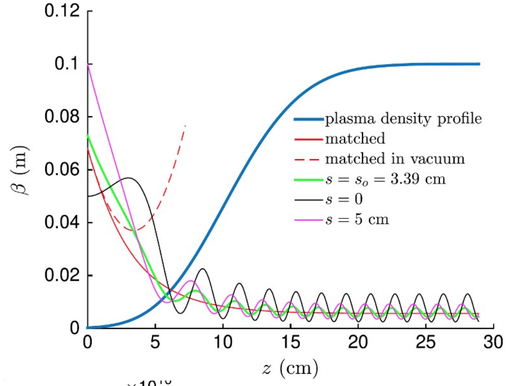

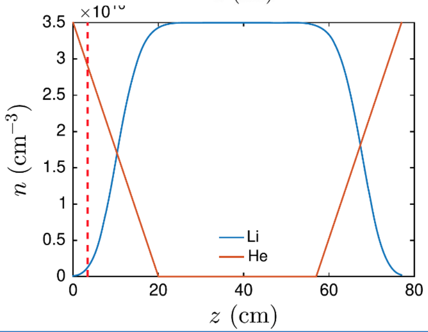

PRAB **23**, 011302 (2020)

MHD software can address plasma system modeling challenges

- Structured plasma systems are well suited for magneto-hydrodynamic modeling
  - Length Scales (cm–scale) far exceed computational feasibility for PIC simulations
  - Duration of evolution (ns) similarly require many hundreds of thousands of steps
  - Quantities of interest (density, temperature, ionization state) are more suited for fluid than kinetic description
  - Established efforts in HEDP community demonstrate viability of these tools for a range of plasma phenomena

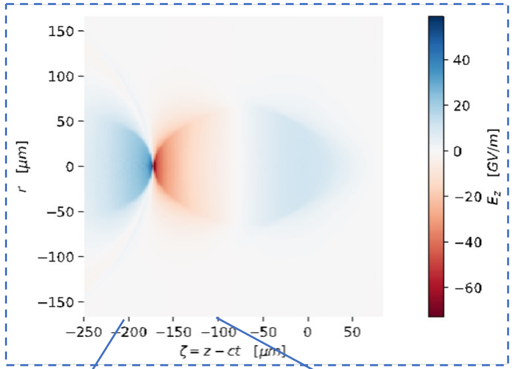

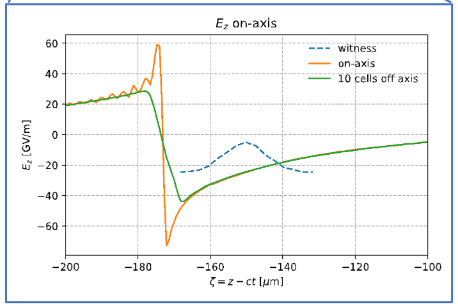

L = 30 cm, τ_e = 1 ns

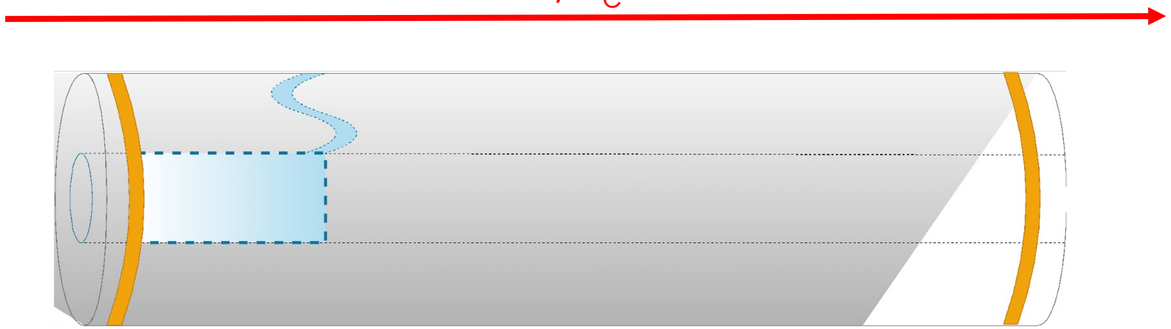

PIC Region of Interest: [500 μm x 500 μm]

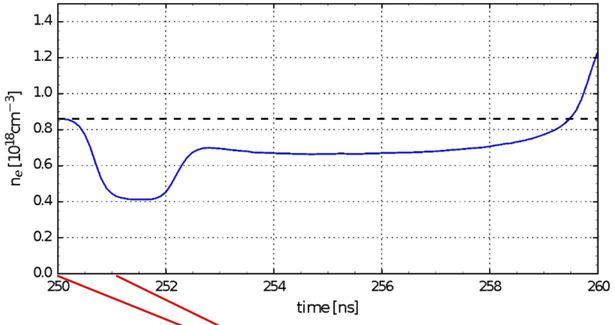

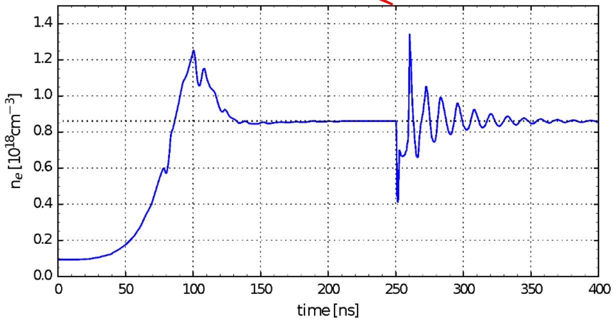

The FLASH Code: a modular, multiphysics tool for plasmas

- Compressible flow evolution on block-structured mesh
  - Compute fluid evolution with convection and other source terms:

$$\left\{\begin{array}{c} \frac{\partial \rho}{\partial t} + \nabla \cdot (\rho \boldsymbol{v}) = 0 \\ \frac{\partial}{\partial t}(\rho \boldsymbol{v}) + \nabla \cdot (\rho \boldsymbol{v}\boldsymbol{v}) + \nabla P_{\text{tot}} = 0 \\ \frac{\partial}{\partial t}(\rho E_{\text{tot}}) + \nabla \cdot [(\rho E_{\text{tot}} + P_{\text{tot}})\boldsymbol{v}] = Q_{\text{las}} - \nabla \cdot \boldsymbol{q} \end{array}\right\}$$

  - 3T representation of fluid (electron, ion, radiation):

$$\left\{\begin{array}{c} \frac{\partial}{\partial t}(\rho e_{\text{i}}) + \nabla \cdot (\rho e_{\text{i}} \boldsymbol{v}) + P_{\text{i}} \nabla \cdot \boldsymbol{v} = \rho \frac{c_{v,e}}{\tau_{ei}}(T_{\text{e}} - T_{\text{i}}) \\ \frac{\partial}{\partial t}(\rho e_{\text{e}}) + \nabla \cdot (\rho e_{\text{e}} \boldsymbol{v}) + P_{\text{e}} \nabla \cdot \boldsymbol{v} = \rho \frac{c_{v,e}}{\tau_{ei}}(T_{\text{i}} - T_{\text{e}}) - \nabla \cdot \boldsymbol{q}_{\text{e}} + Q_{\text{abs}} - Q_{\text{emis}} + Q_{\text{las}} \\ \frac{\partial}{\partial t}(\rho e_{\text{r}}) + \nabla \cdot (\rho e_{\text{r}} \boldsymbol{v}) + P_{\text{r}} \nabla \cdot \boldsymbol{v} = \nabla \cdot \boldsymbol{q}_{\text{r}} - Q_{\text{abs}} + Q_{\text{emis}} \end{array}\right\}$$

- Species-based characterization of state and transport:
  - Resistivity and conduction models describe heating and dissipation
  - Tabulated EOS for accurate internal energy and ionization calculations
- Energy deposition capabilities:
  - Laser deposition via Inverse Bremsstrahlung
  - Heat exchange for equilibration of different components
- Magnetohydrodynamics via unsplit, staggered mesh scheme
  - Second order predictor-corrector scheme
  - Explicit integration introduces time step limitations

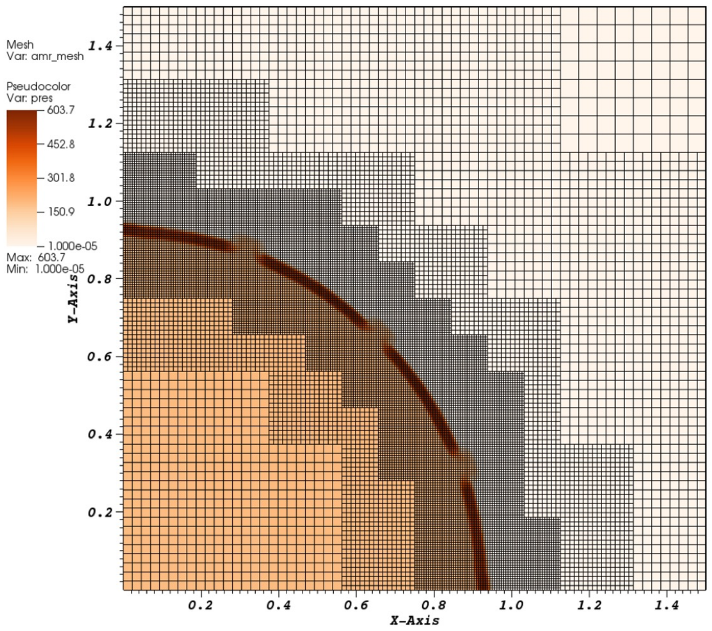

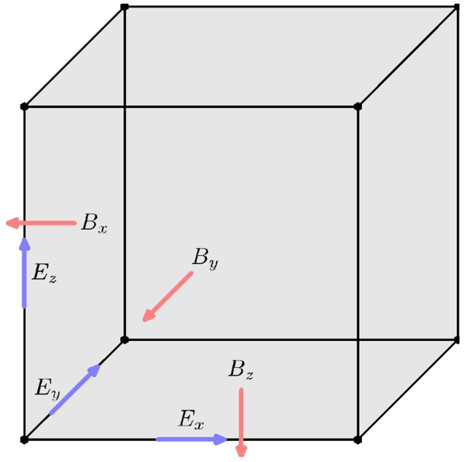

The FLASH code: organization and structure

- Modular, hierarchical structure permits selective inclusion of relevant “units”
  - *Infrastructure*
    - Grid and memory management
    - I/O, checkpoint, restarts
    - Runtime parameters
  - *Physics*
    - Hydro/MHD
    - Material properties
    - Particle features
    - Deposition/sources
  - *Monitoring*
    - Logging, profiling, debugging
  - *Simulation*
    - User customization
    - Test problems
  - *Driver*
    - Initialize and evolve code
    - Compute/coordiante timesteps

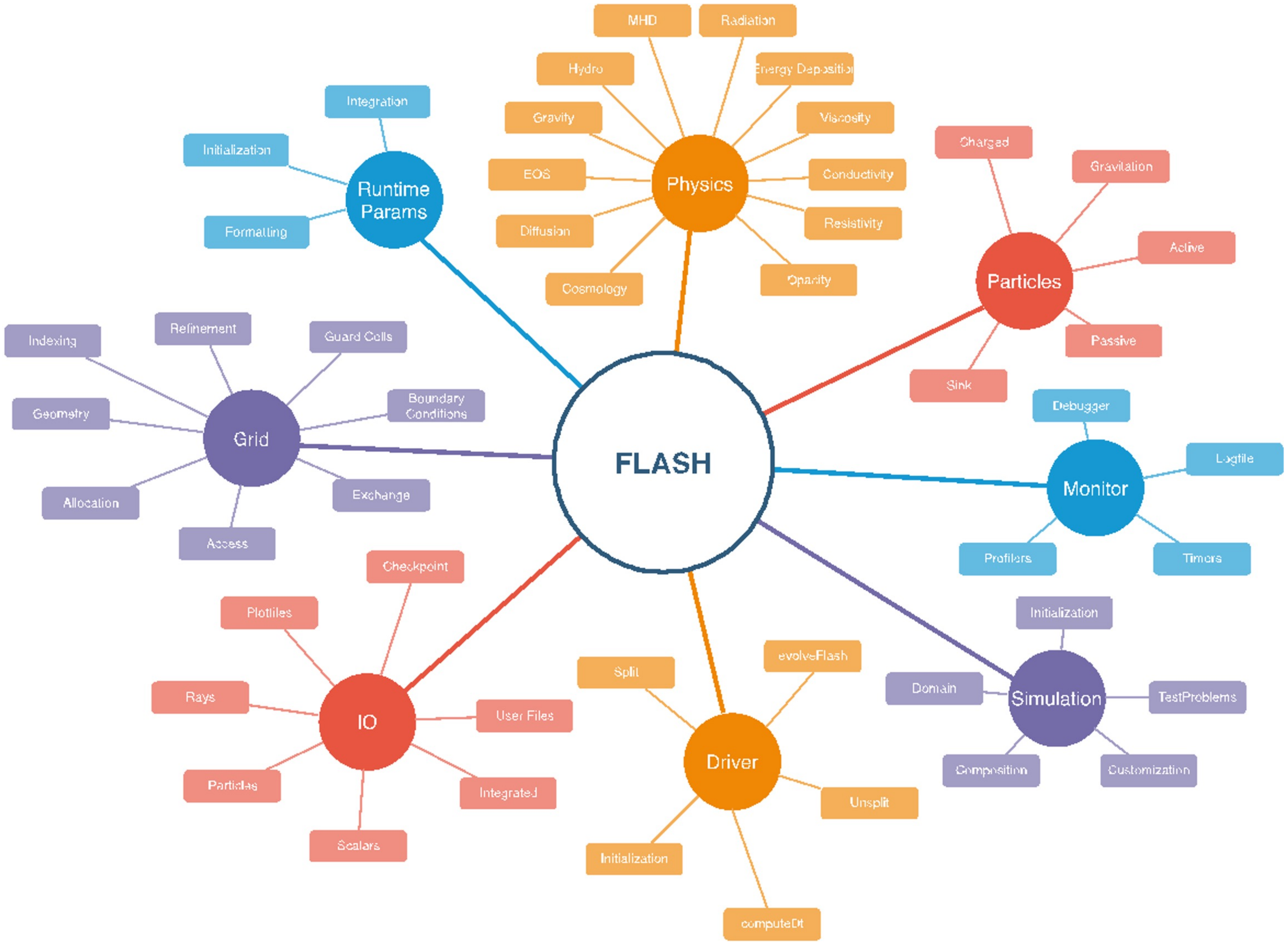

Equation of State – Multi-temperature, Multi-species Tabulated

- Tabulated equation of state provides closure, and corresponding radiation diffusion coefficients
  - Code requires a pair of inputs (density, temperature, pressure, internal energy) to search a lookup table
    - Our simulations use density and temperature to determine internal energies and ionization
    - Multi-temperature mode produces call for each component (electron, ion, radiation)
  - Multi-species mode returns separate results for each material, for use with mixed-species fluids (via separate tables)
  - *Tables must be provided by users! IONMIX, SESAME, PrOpacEOS*
- Table range and resolution are critical to resolving dynamics, especially at early times
  - Extending tables to low temperatures is challenging
    - Extrapolation may be used to include these regions
  - Solver difficulties often manifest in EOS errors
    - Negative internal energies produced by large gradients in density, pressure, or due to large ratio of kinetic to internal energy

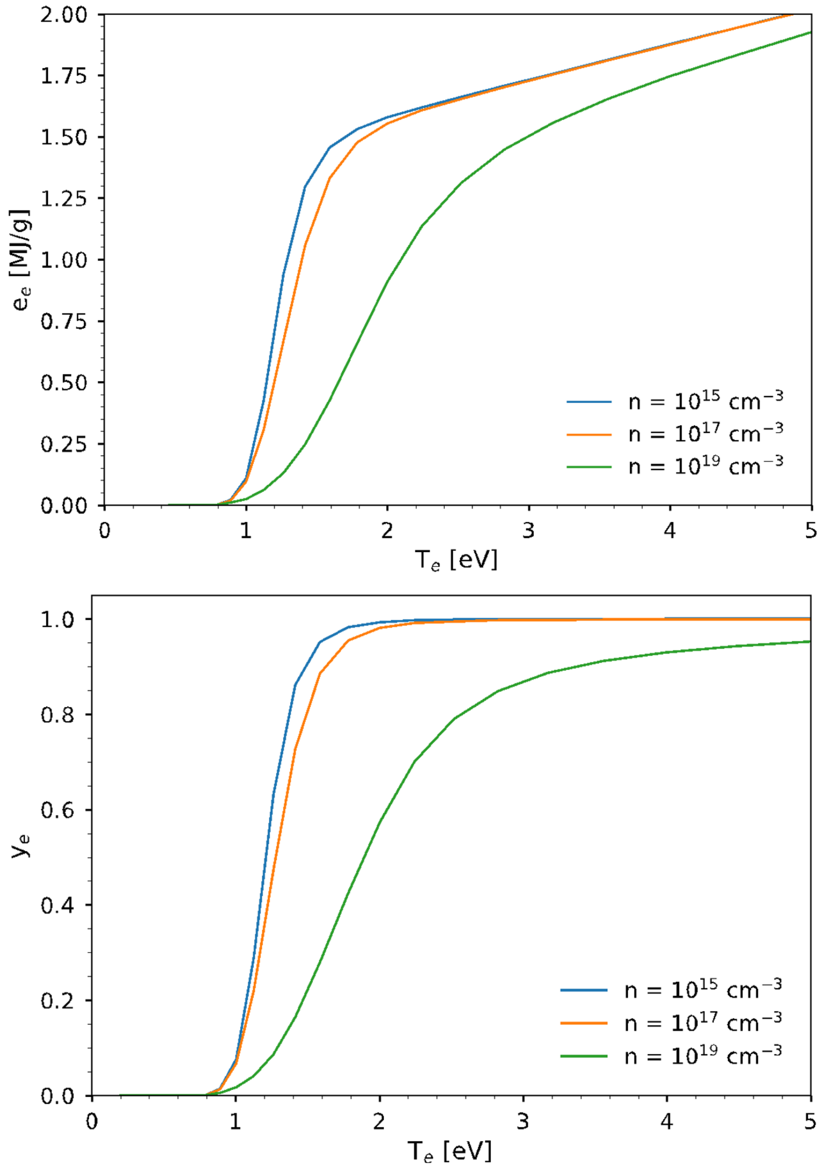

Energy Deposition via Inverse Bremsstrahlung and Ray-Tracing

- Laser propagation is computed via ray tracing, with assumption of instantaneous traversal

$$\mathbf{v}(t) = \mathbf{v}_0 - \frac{c^2}{2n_c}\nabla n_e(r_0)t \qquad \mathbf{r}(t) = \mathbf{r}_0 + \mathbf{v}_0 t - \frac{c^2}{4n_c}\nabla n_e(r_0)t^2$$

  - System response (density/index of refraction) is assumed to be slow compared to ray transit
  - At each step, all rays are transported until they exit domain or are absorbed by medium
  - Temporal profile of laser is determined by a piecewise composition of sequence of laser power designations
  - Transverse profile is determined by choice of lens and target dimensions and cross-sectional representation
    - Rays are then populated transversely across a local grid covering the lens
    - Power is distributed to reflect the chosen cross-section
  - For anisotropic interactions, a quasi-3D ray tracing algorithm can be used
    - Divide cylindrical space into identical wedges
- Laser energy deposition is modeled via Inverse Bremsstrahlung

$$\frac{dP}{dt} = -\nu_{ib}(t)P \qquad \nu_{ib}(r,t) = \frac{4}{3}\left(\frac{2\pi}{m_e}\right)^{1/2}\frac{Ze^4}{n_c k_B^{3/2}}\frac{n_e[r(t)]^2 ln\Lambda[r(t)]}{T_e[r(t)]^{3/2}}$$

  - Significantly reduced efficacy at low densities and high temperatures
  - Additional energy deposition *could* be hand-coded via `simulation_adjustEvolution` routine

Anisotropic Magnetic Resistivity Model – Davies & Wen

- Strong azimuthal magnetic field motivates use of anisotropic conduction, resistivity formalisms

$$\frac{\partial \mathbf{B}}{\partial t} = \nabla \times \left(\mathbf{v}_{\text{eff}} \times \mathbf{B}\right) - \nabla \times \eta_{\|} \nabla \times \mathbf{B} + \nabla \beta_{\|} \times \nabla T_e + \frac{\nabla P_e \times \nabla n_e}{e n_e^2}$$

$$\mathbf{v}_{\text{eff}} = \mathbf{v} - \left(1 + \delta_{\perp}\right) \frac{\mathbf{j}}{n_e e} - \delta_{\wedge} \frac{\mathbf{j} \times \mathbf{b}}{e n_e} + \gamma_{\|} \left(\nabla T_e \times \mathbf{b}\right) - \gamma_{\perp} \nabla T_e$$

- Implemented anisotropic resistivity model based on Davies & Wen*
    - Significant improvements to Spitzer model via reduced resistivity and increased field penetration
    - Slight increase in resistivity vs alternative Ji & Held model

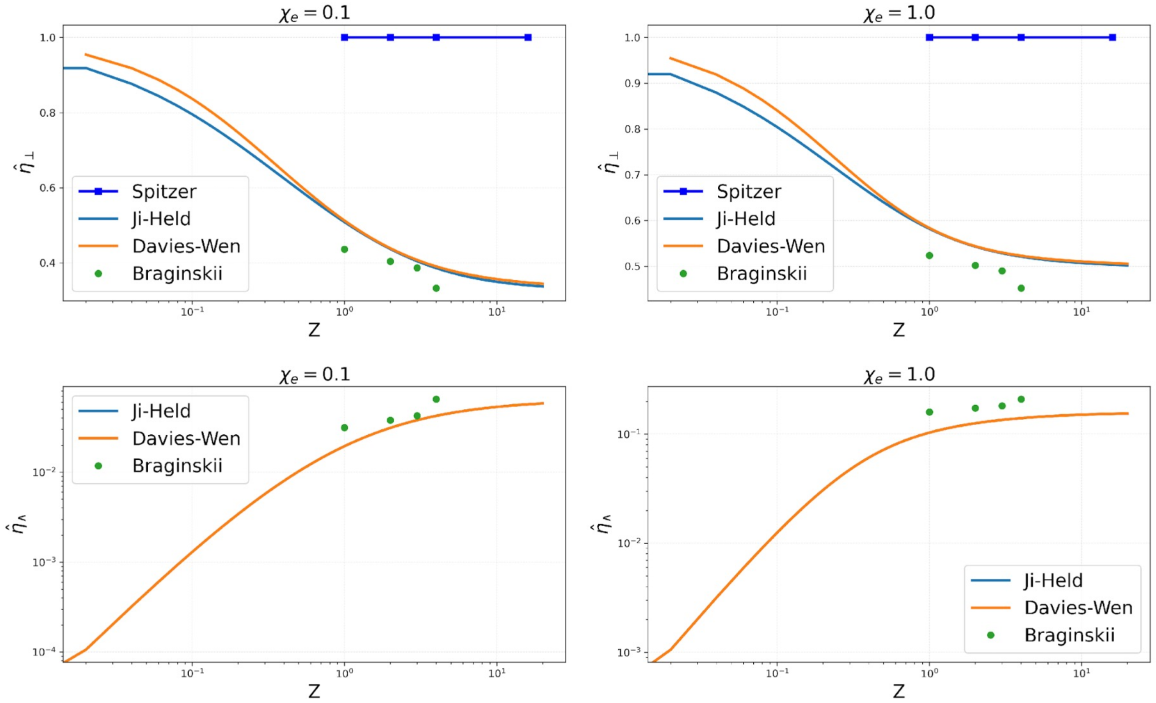

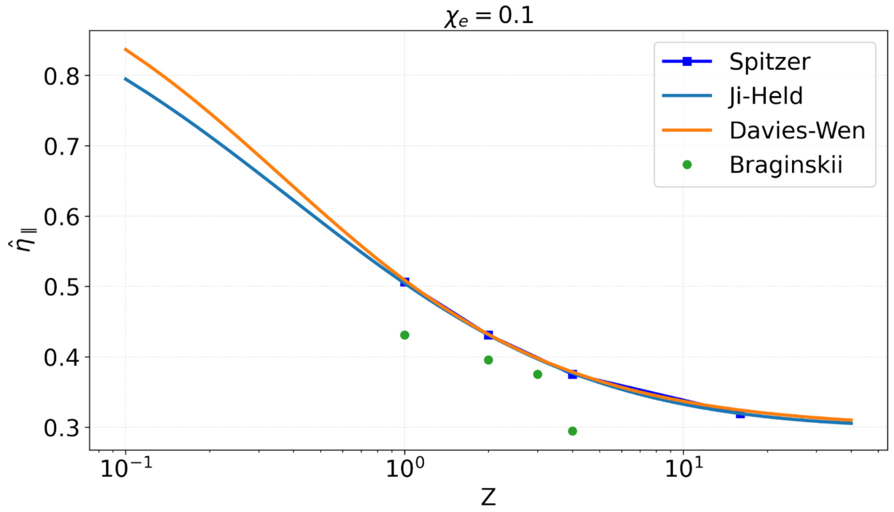

*Physics of Plasmas **28**, 012305 (2021)

Anisotropic Thermal Conduction Model – Ji & Held

- Conduction is also anisotropic, resulting from azimuthal magnetic field

$$\rho c_v \frac{\partial T}{\partial t} = \nabla \cdot \left(K_\parallel \mathbf{b}(\mathbf{b} \cdot \nabla T) + K_\perp \mathbf{b} \times (\nabla T \times \mathbf{b}) + K_\wedge (\mathbf{b} \times \nabla T) \right)$$

- Implemented an anisotropic thermal conduction model, based on Ji & Held*
  - Significant corrections to Braginksii at high magnetization and ionization
  - Enhanced conduction at low magnetization as compared with Epperlein & Haines model

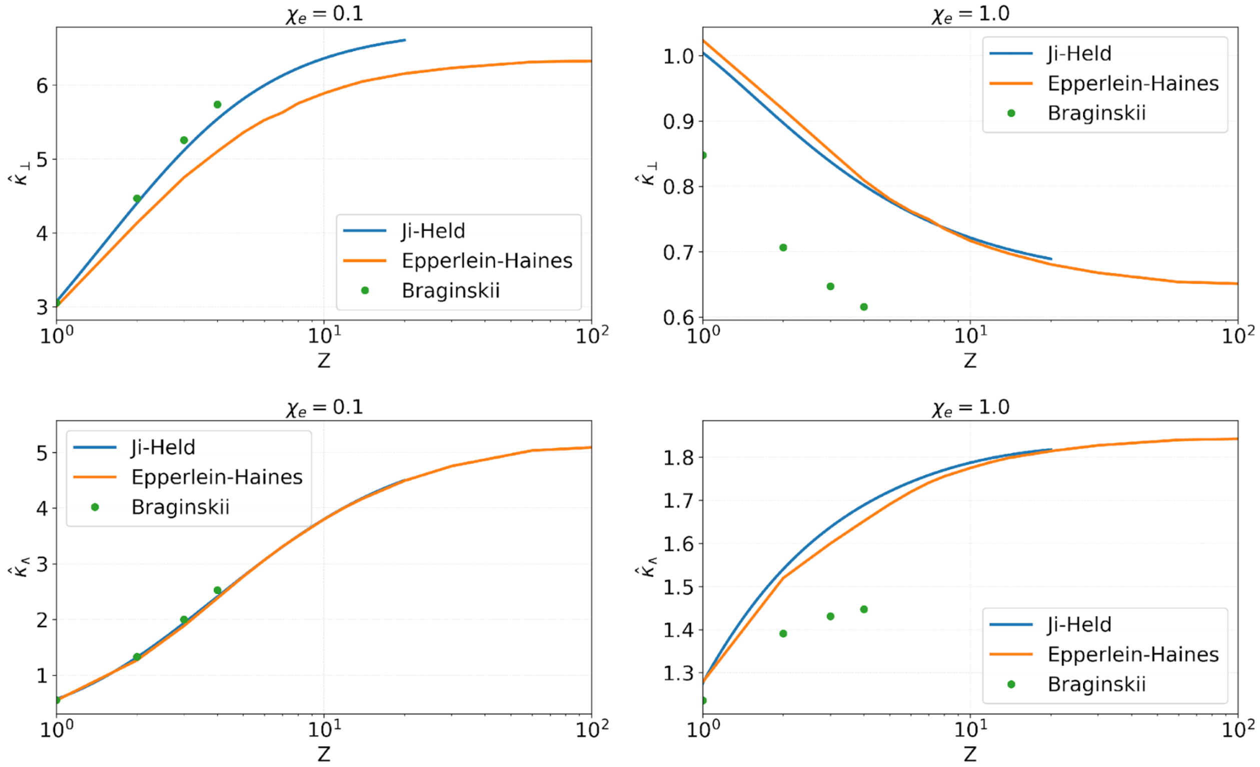

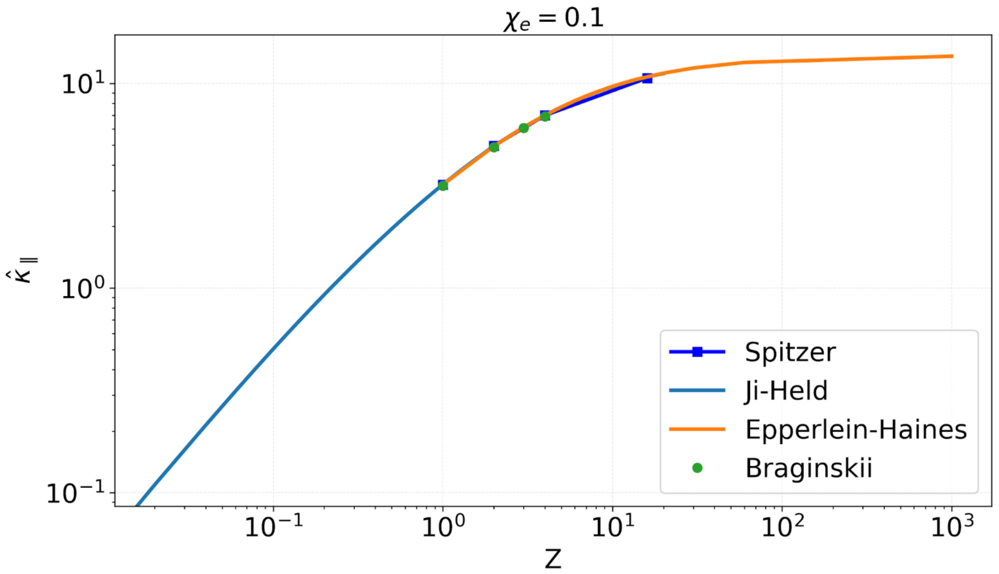

*Physics of Plasmas **20**, 042114 (2013)

Capillary Discharge Representations

- Domain boundary is capillary wall:
  - Set boundary conditions for magnetic field based on Ampere's Law
  - Set thermal conductivity at boundary (Neumann condition)
  - Simple, but only works for conformal capillary geometries

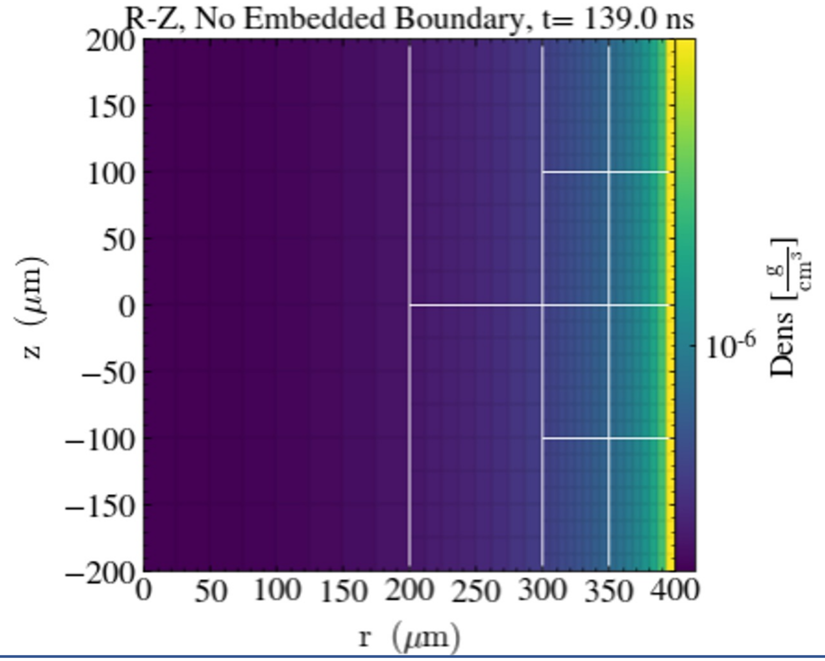

- Embedded capillary wall:
  - Wall material (Al_2O_3) is explicitly included in domain
  - Magnetic field condition is applied at interface of capillary wall via similar calculation
  - Conductivity and resistivity are computed self-consistently throughout domain
  - Wall material is labelled as a `BDRY_VAR`: proper diffusion but no fluid motion
  - Refinement level can be reduced within wall region
  - Can be used to model entire structure, but supply channels require high resolution, as do more complex shapes

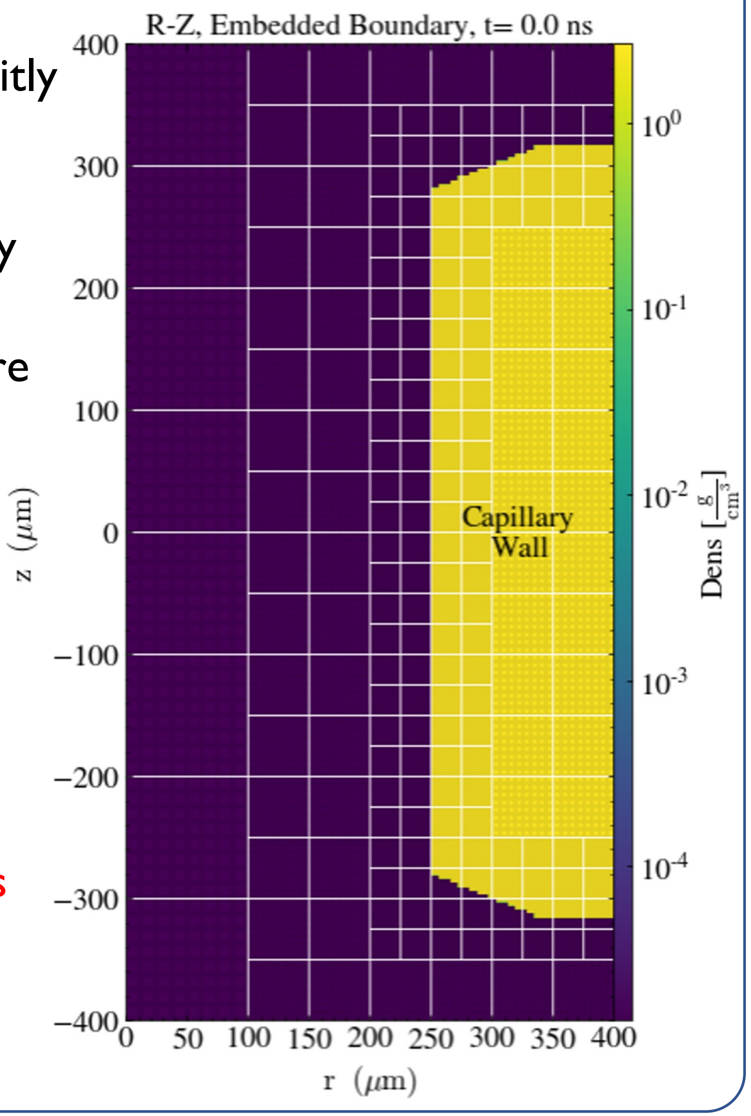

Specifying the discharge current

- Discharge current is represented by magnetic field at capillary wall
  - Ampere's law uniquely specifies the magnetic field from current within capillary
  - Electrons preferentially heated, while ions equilibrate via heat-exchange
- Time dependent boundary condition enables flexible current profile
  - Analytic representation or tabulated values from external file
- Extensible to alternative cross-sections

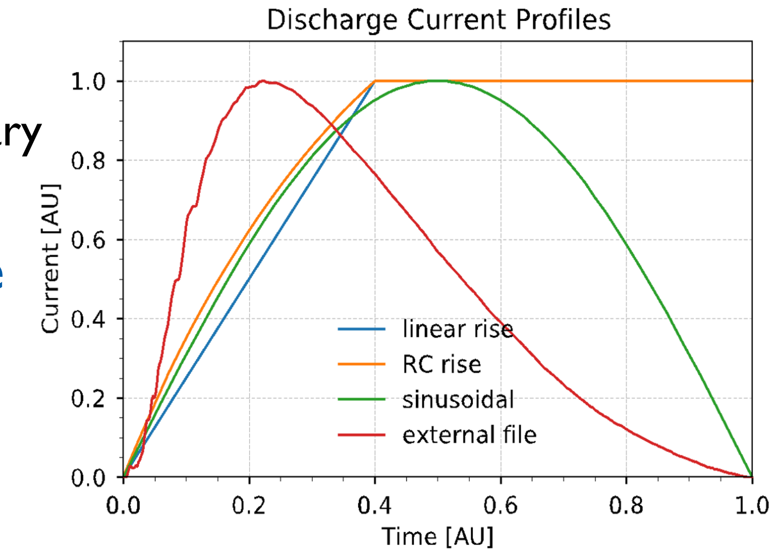

$$B_x = \frac{\mu_0}{2\pi} \int \int \frac{\hat{z} \times \hat{x}}{r} dx\, dy = \frac{\mu_0}{2\pi} \int_{-w/2}^{w/2} \int_{-h/2}^{h/2} \frac{-\hat{x}\sin\theta + \hat{y}\cos\theta}{\sqrt{(x_0 - x)^2 + (y_0 - y)^2}} dx\, dy$$

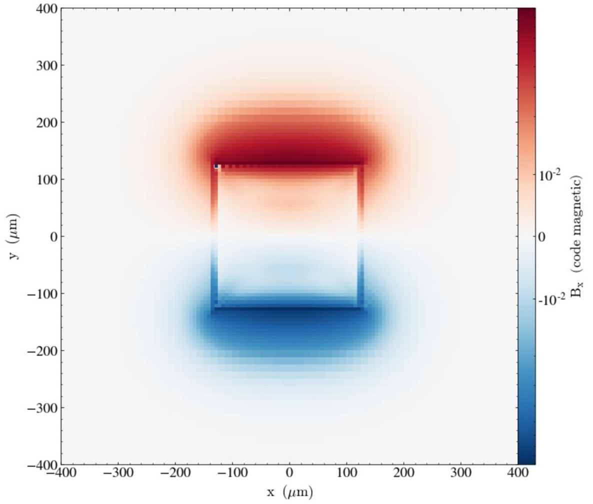

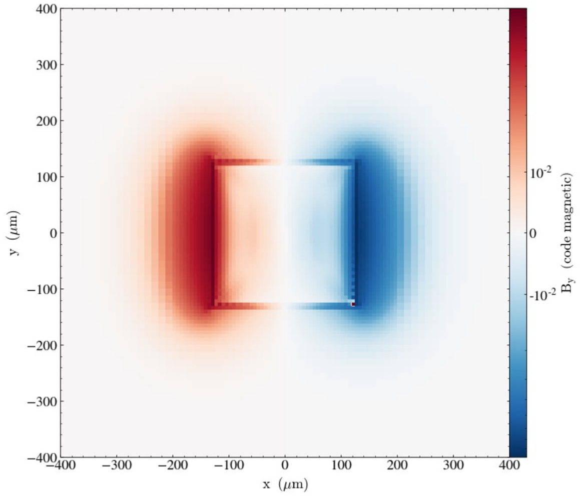

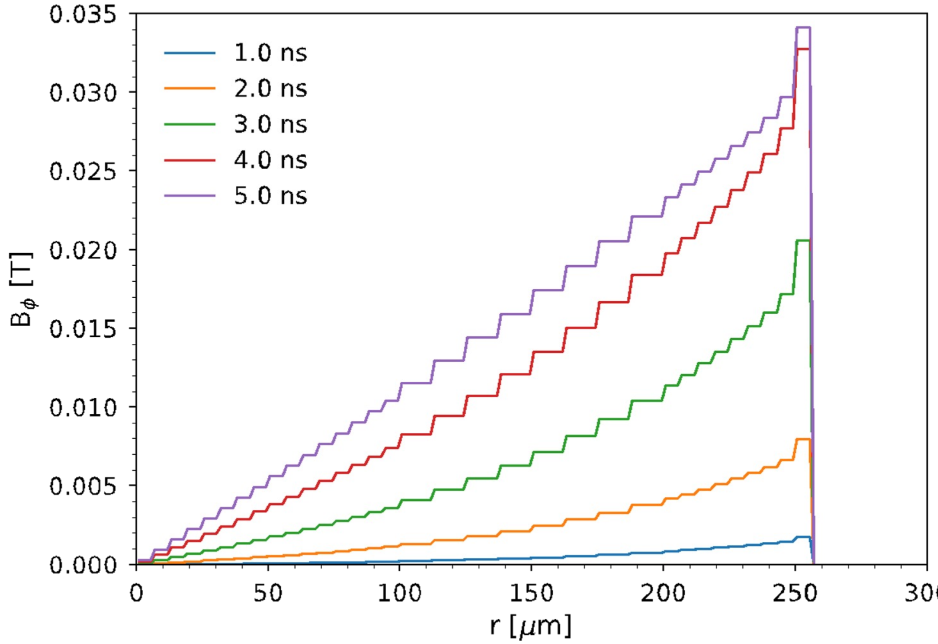

Capillary dynamics characterized by a three-phase evolution

1. Ohmic heating and ionization from discharge
    - Magnetic field penetration drives heating of the gas
    - Heating and ionization are largely uniform radially
    - Persists until nearly full ionization
    - ~100s of ns duration, density & discharge-dependent
2. Re-distribution of plasma by thermal dissipation
    - Thermal conduction produces temperature gradient
    - Plasma re-organizes in response to gradients
    - ~10s of ns duration, density & species dependent
3. Quasi-steady-state channel formation
    - Balance between Ohmic heating along channel and conductive cooling at capillary wall
    - Radial inversion in density and temperature
    - Density forms a near parabolic channel with on-axis peak in temperature
    - ~100s of ns duration, discharge-dependent

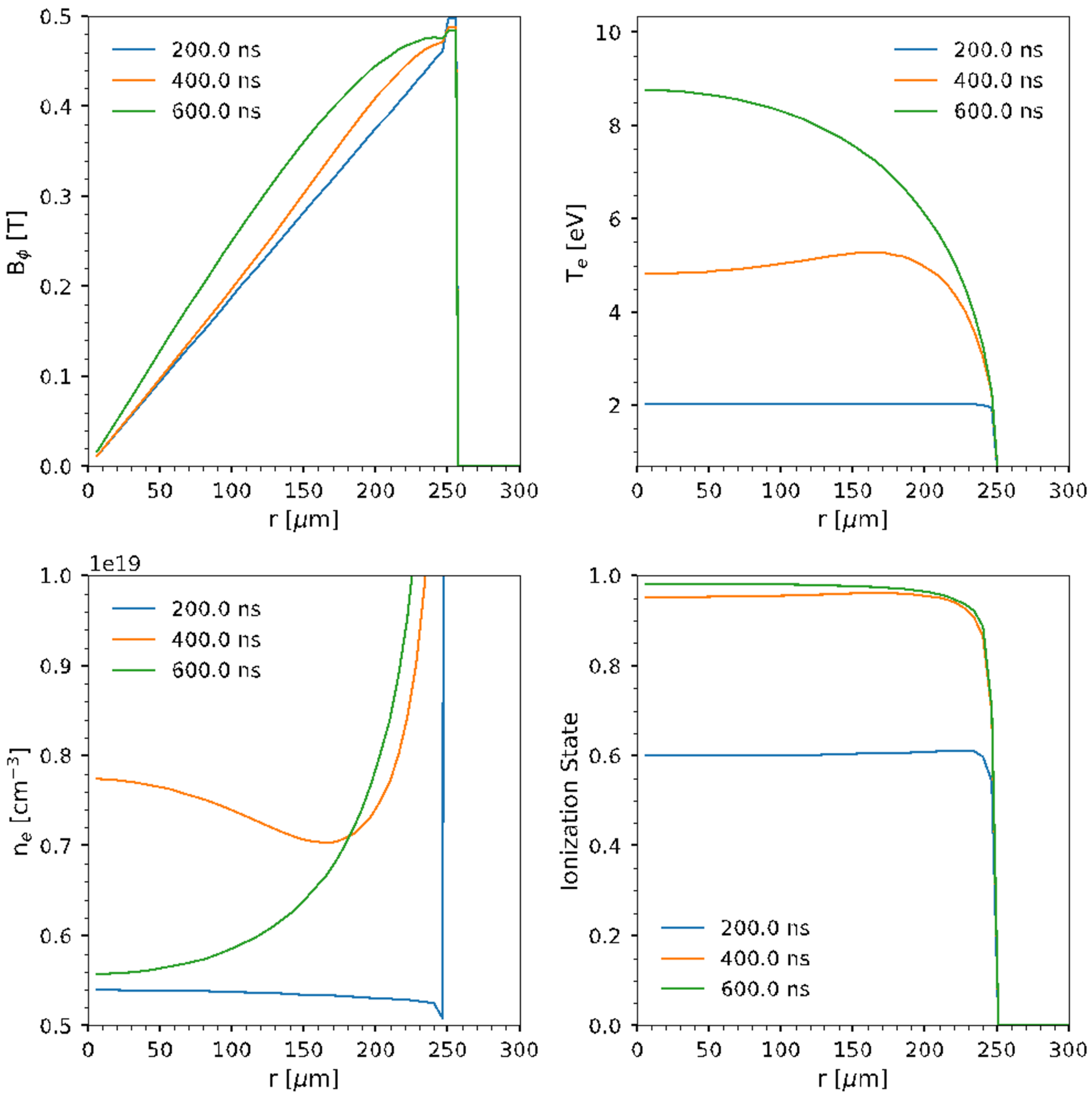

Choice of transport model affects heating rates

- Significant variations in the rate of heating and ionization
- Spitzer model heats more quickly and to a higher peak
  - Spitzer models heat more **~20% more quickly** and achieve **20% higher peak temperatures** for Hydrogen and Argon
- Very similar channel densities are achieved
  - But temperature deviation has significant implications for the laser heater efficacy for sub-channel formation

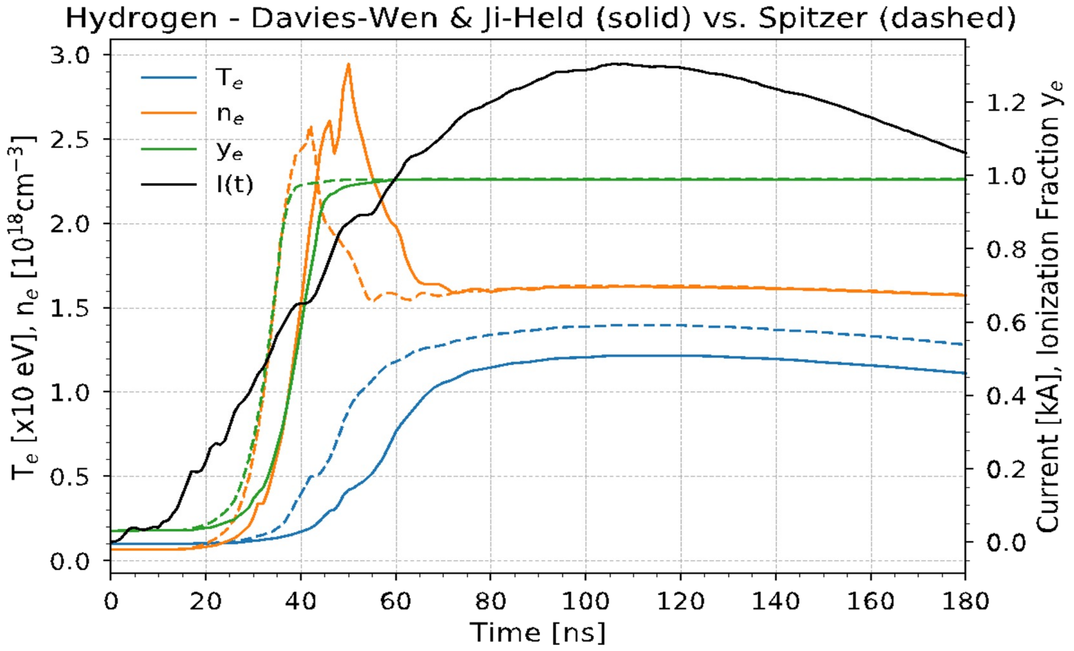

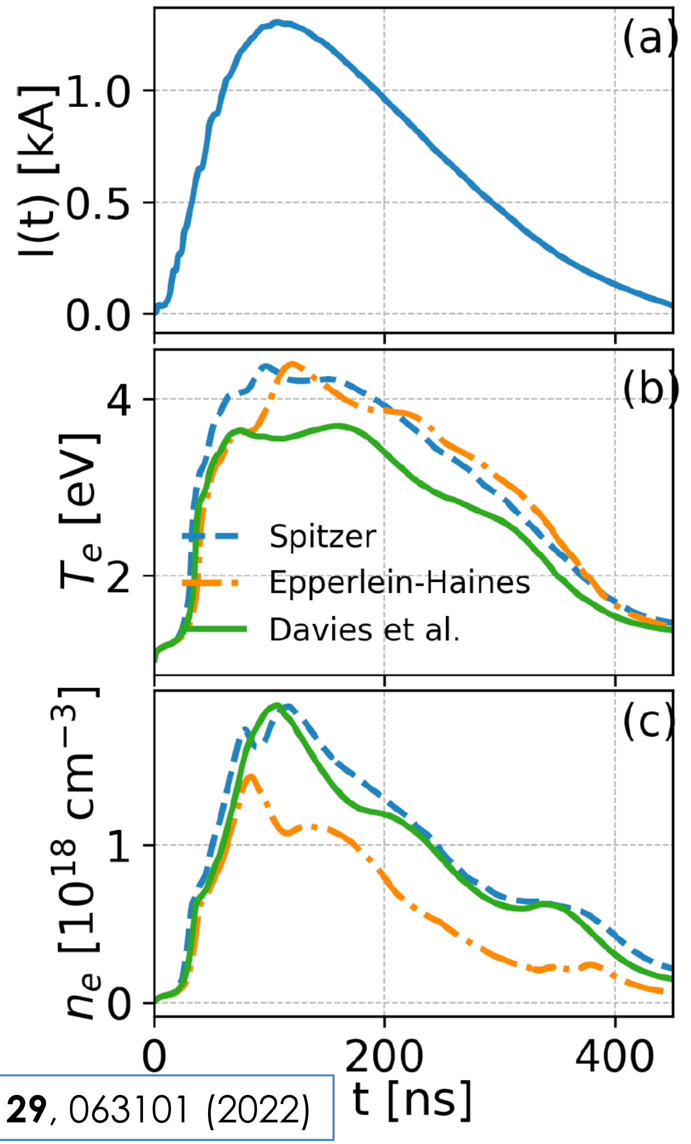

Physics of Plasmas **29**, 063101 (2022)

Three-Dimensional simulation show good agreement with R-Z

- 3D simulations reproduce essential dynamics
  - Reduced refinement (3x vs. 4x) halves resolution compared with 2D
  - Magnetic field penetration within channel is comparable
  - Resulting heating and ionization levels are consistent through 100 ns
    - Some reduction in temperature on axis as compared with 2D runs
- Some remaining considerations
  - Magnetic field dissipation is reduced in the wall, but temperature is consistent
  - Small asymmetries in dissipation along azimuthal angle

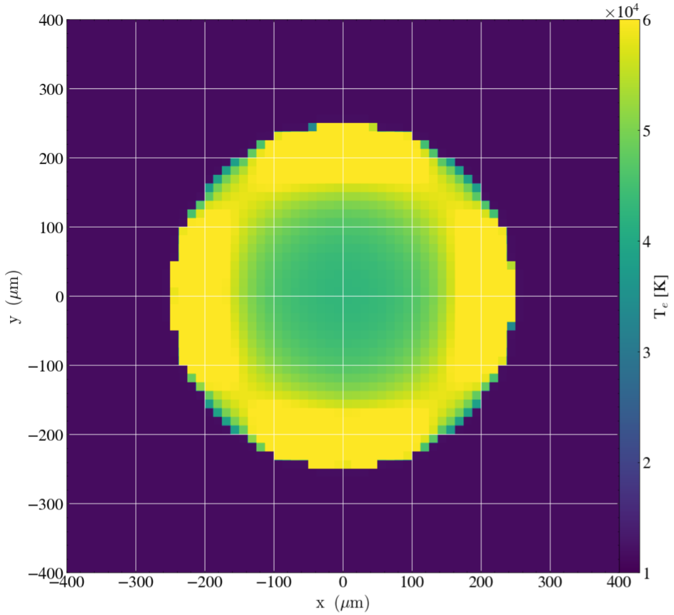

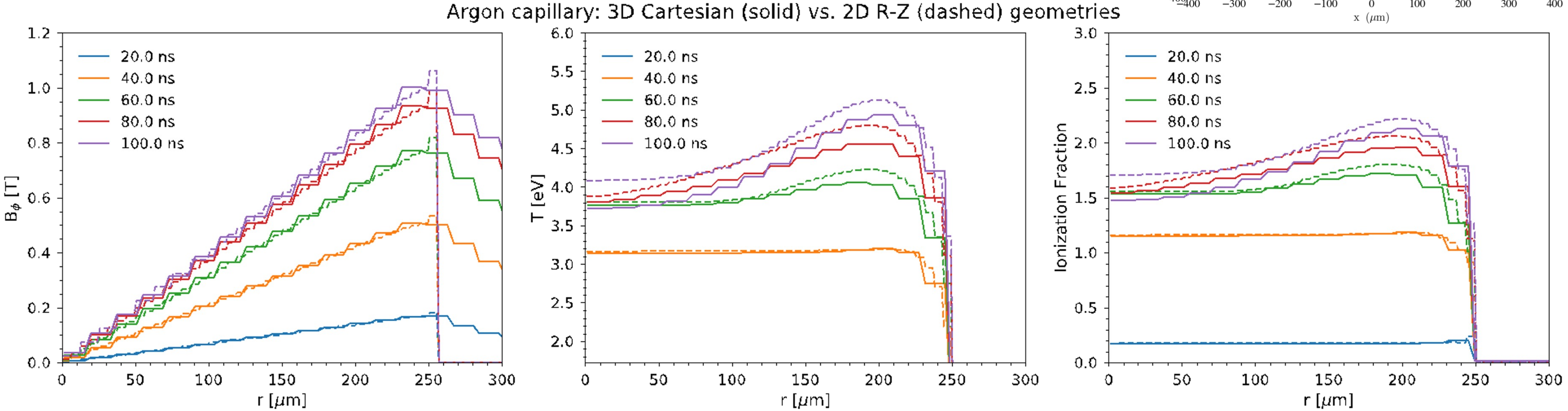

Laser energy deposition enables sub-channel formation

- Coupling depends on plasma density and transverse gradient
  - Matched spot size follows capillary radius and channel depth
  - Aperture and plasma density limit matched spot size by constraining r_0.
- Secondary laser enhances channel depth on axis
  - Example: Reduction in spot size from >100 micron to ~73 micron
  - Density minimum happens ~6 ns into deposition
- Absorption is greater at low temperatures, high densities – timing is important!

$$W_0 \approx \left(\frac{r_0^2}{\pi r_e \Delta n} \right)^{1/4}$$

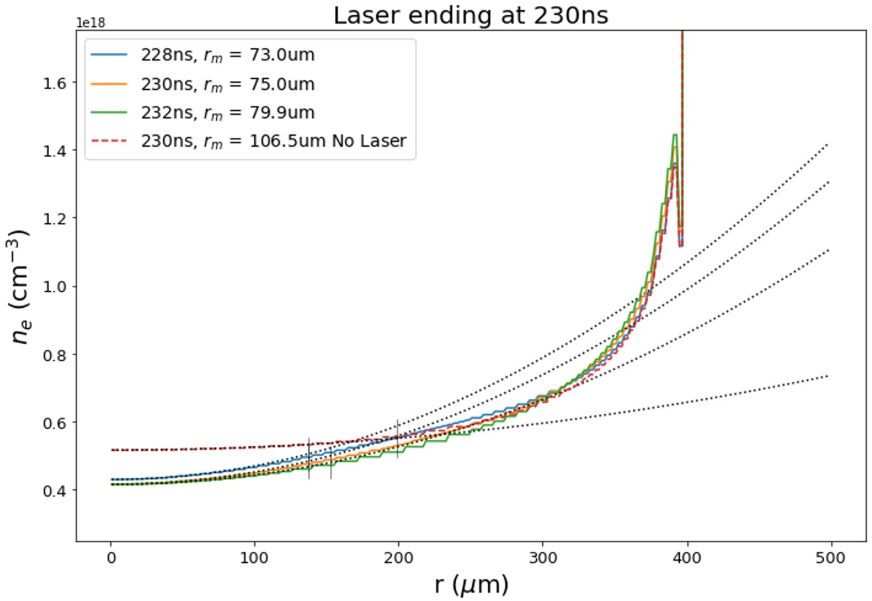

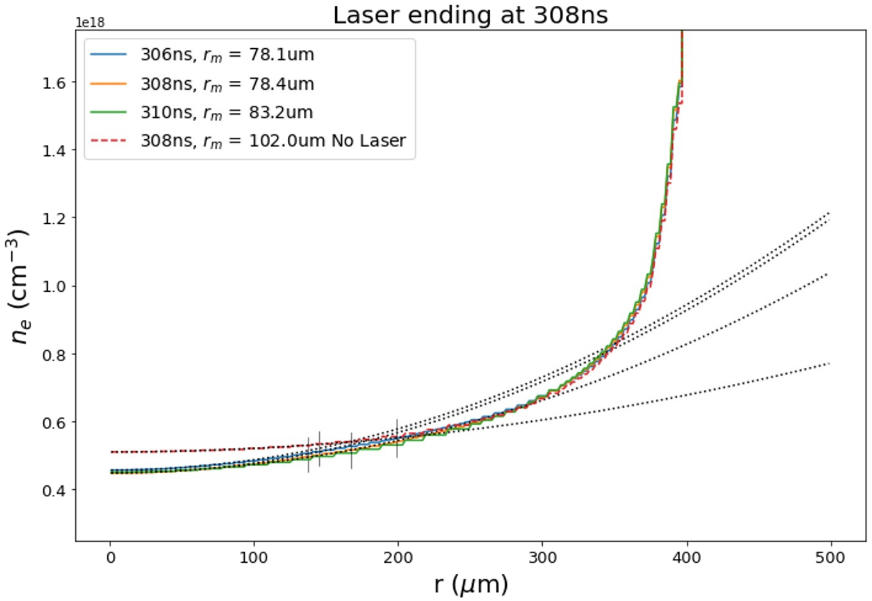

Sub-channel formation is sensitive to underlying conditions

- Peak current, peak temperature, and minimum laser efficacy are well correlated
  - Launching the heater laser at peak current and temperature is least effective (50% lower relative reduction)
- However, slight asymmetry in temperature favors earlier laser timings
  - Launching the heater laser ahead of the peak current improves relative channel depth (10-15% improvement)

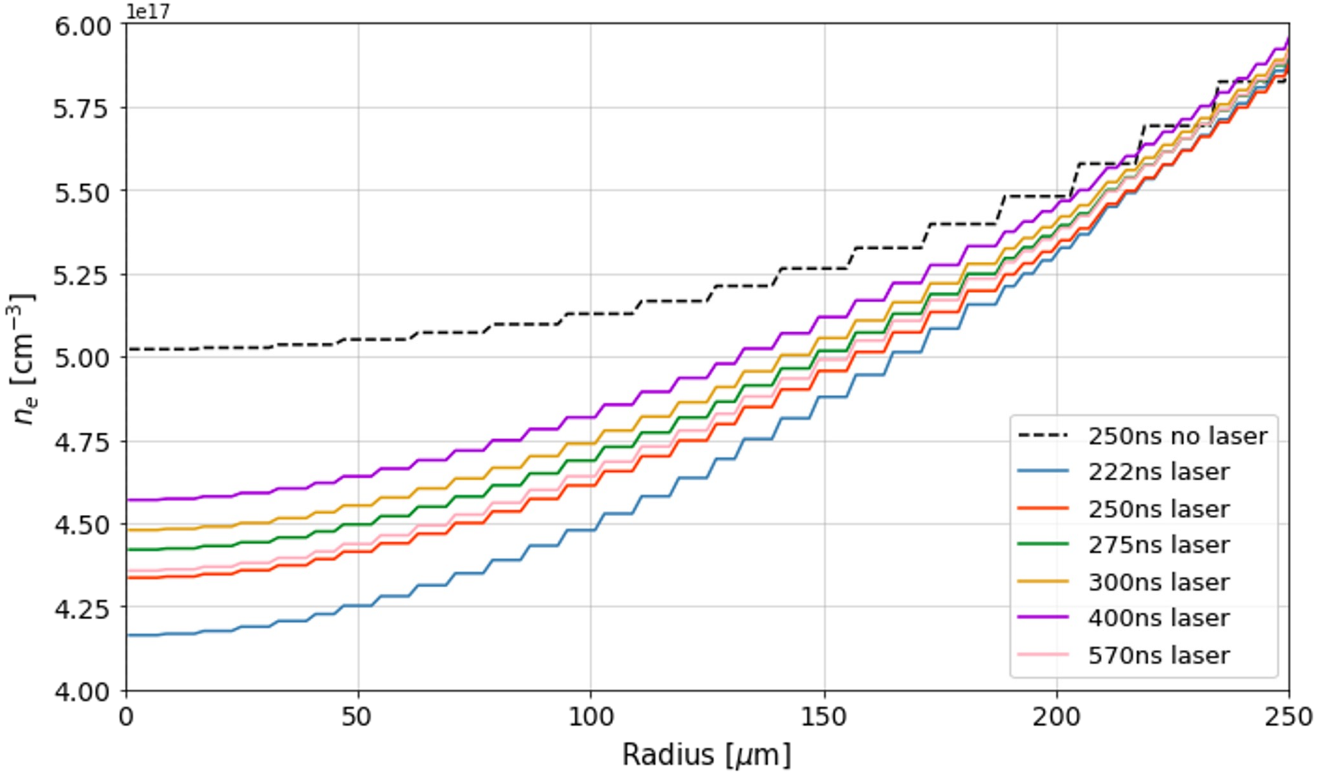

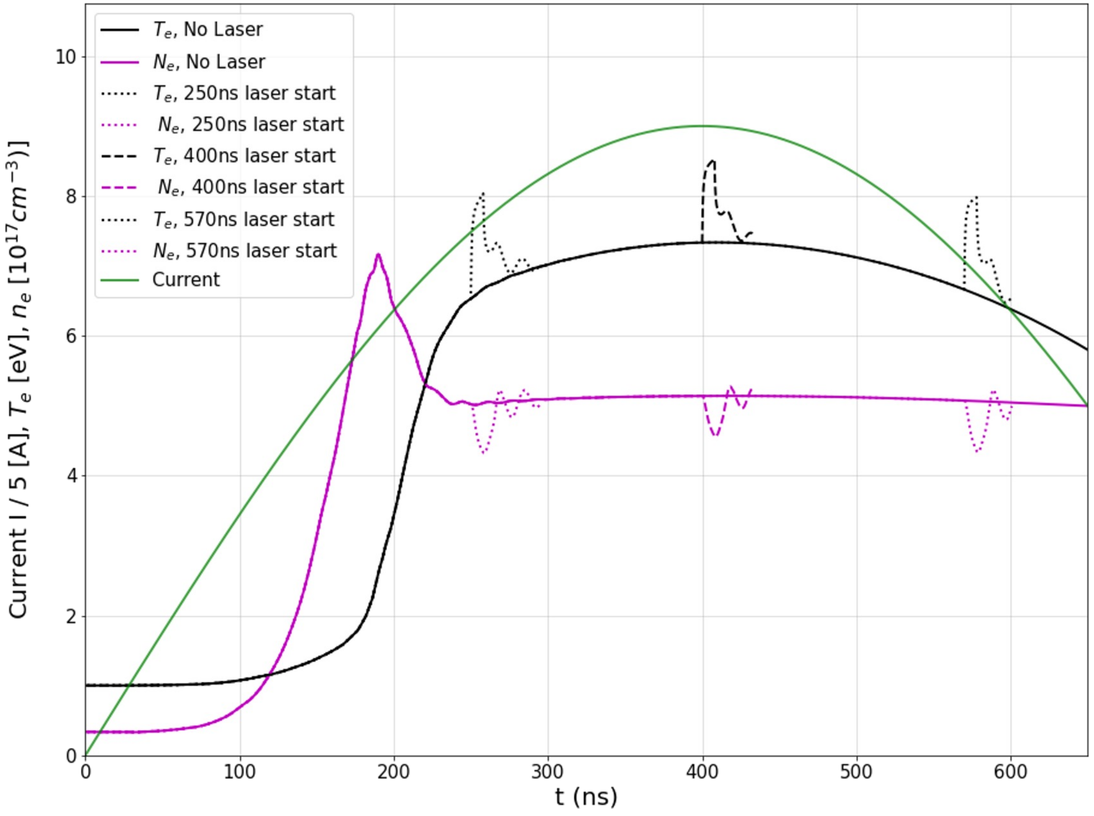

Expected field aberrations seen in active plasma lenses

- Channel formation re-distributes plasma
  - Resistivity varies with plasma temperature
  - Magnetic field penetration adapts to new profile
  - Resulting nonlinearity approximated via J-T profile, yielding nonlinear fit as a function of transport model temperature dependence
- Argon magnetic field profile maintains quasi-linearity over hundreds of ns
  - Despite significantly lower plasma densities, Argon more effectively absorbs and dissipate energy
  - However, ionization dynamics differ substantially, resulting in density and temperature inversion
- Simulations capture dynamics of ionization, temperature, and density inversion
  - Although *more linear* than Helium, near-axis gradients are ~50% lower in Argon
  - Dynamics are sensitive to transport model and code implementation

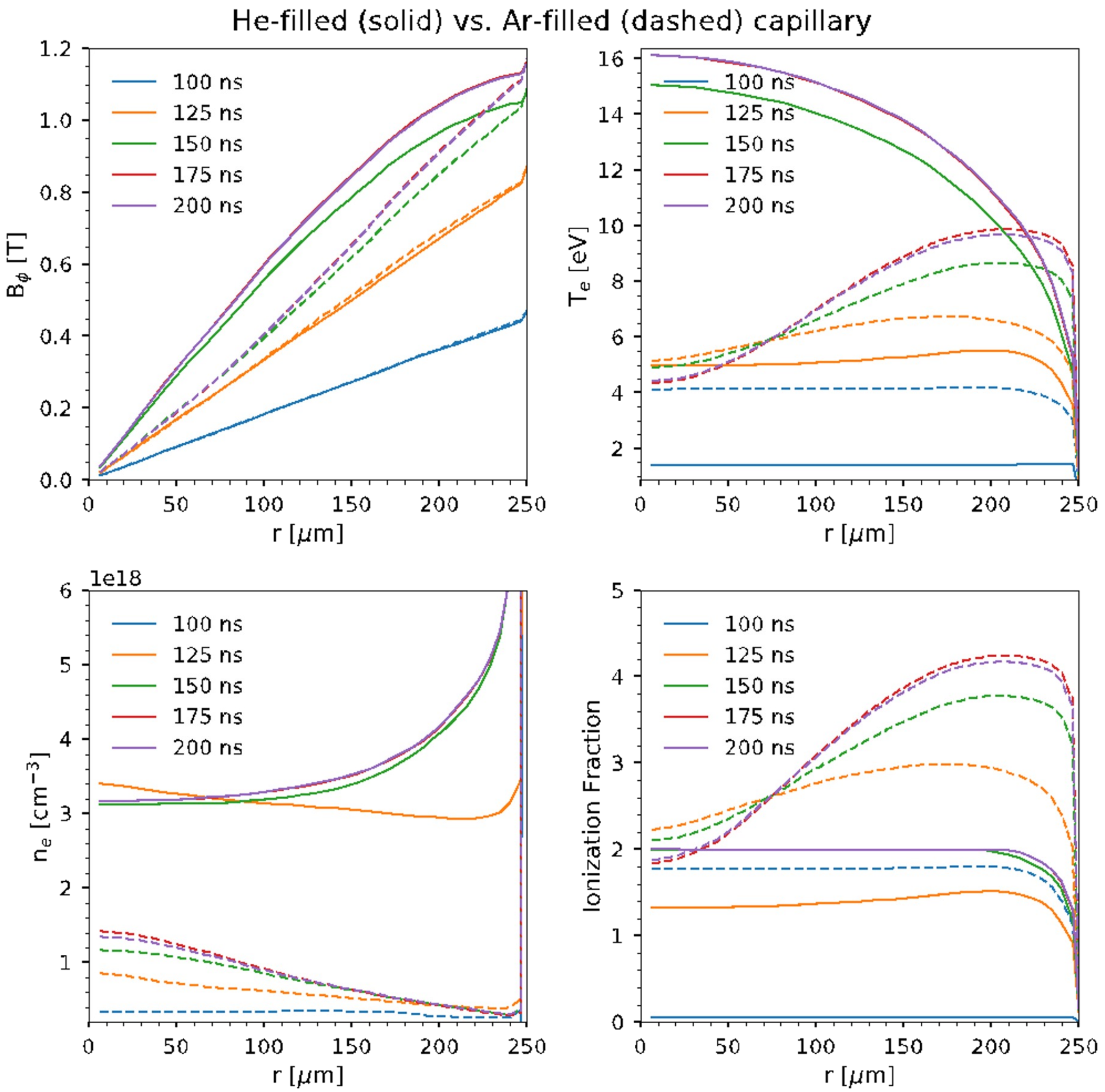

Optically-field-ionized ((H)OFI) channels support narrower channels

- Intense laser drives local heating and ionization in cold gas
  - Channel results from radial hydrodynamic expansion
  - Extended focus permits meter-scale channels
- Prior modelling leverages hydro codes, including FLASH
  - Great progress made in modeling and demonstration
    - R.J. Shaloo et al. PRAB, **22**, 041302 (2019)
    - A. Picksley et al. Phys. Rev. E. **102**, 053201 (2020)
    - B. Miao *et al.*, Phys. Rev. Lett., **125**, 074801 (2020)
  - *Simplifying assumptions:*
    - *Energy deposition described through designation of internal energy, typically based on the first ionization energy*
    - *No explicit laser propagation model – deposition profile is pre-tabulated*
- Our recent work revisits these efforts with a few aims
  - Reproduce essential dynamics
  - Incorporate improved transport models
  - Evaluate EOS and opacity influence
  - Enhance performance
  - Explore parametric optimization

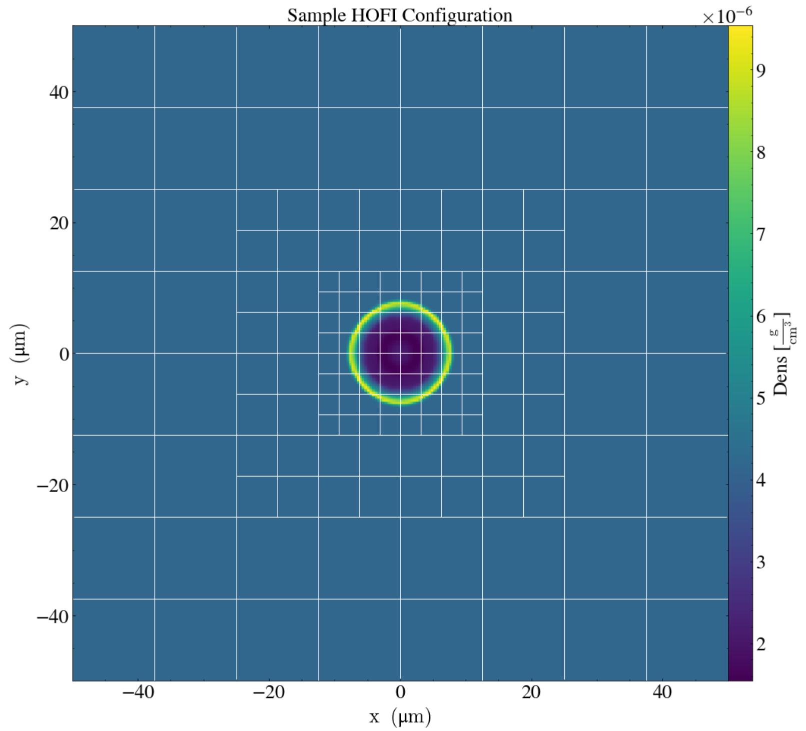

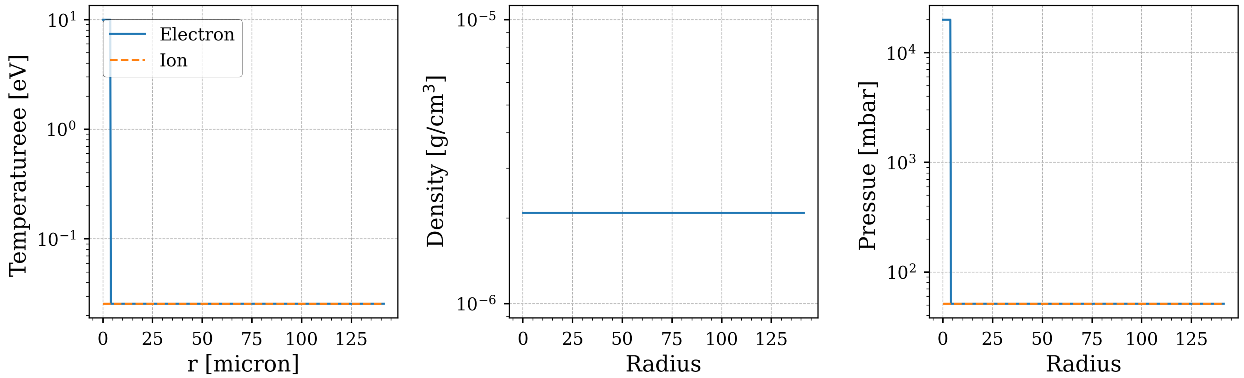

Initial HOFI simulations with FLASH show promise

A. Picksley et al. Phys. Rev. E. **102**, 053201 (2020)

- Simulations reproduce essential dynamics, with caveats
  - Temperature and density dynamics show good agreement
  - Significant discrepancies in ionization state resulting from choice of equation of state and initial conditions (temperature, density)
  - Dynamics at low temperature are sensitive – extending models to low plasma densities and temperatures is an active area of research

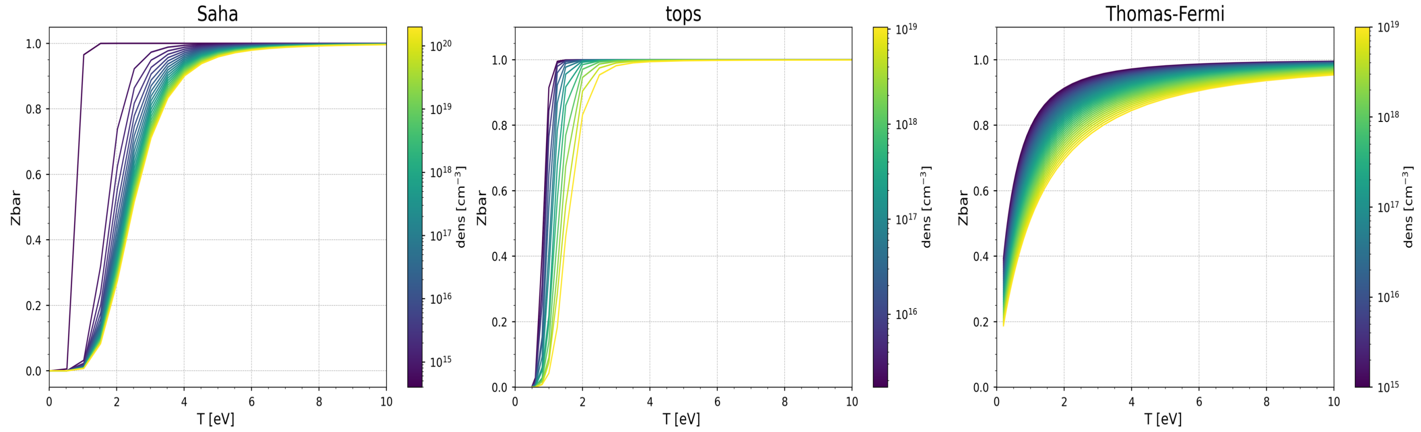

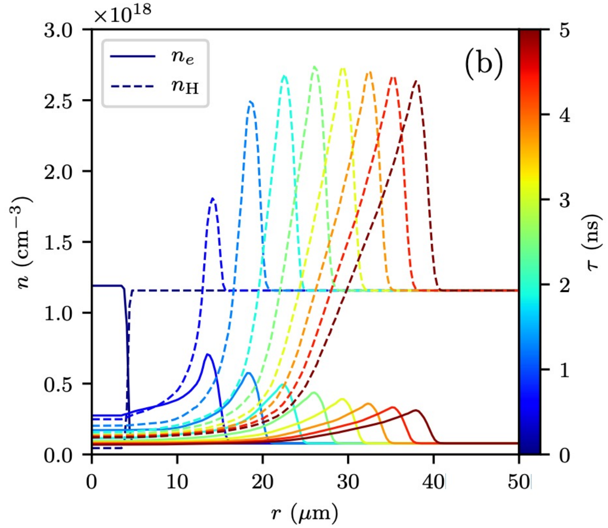

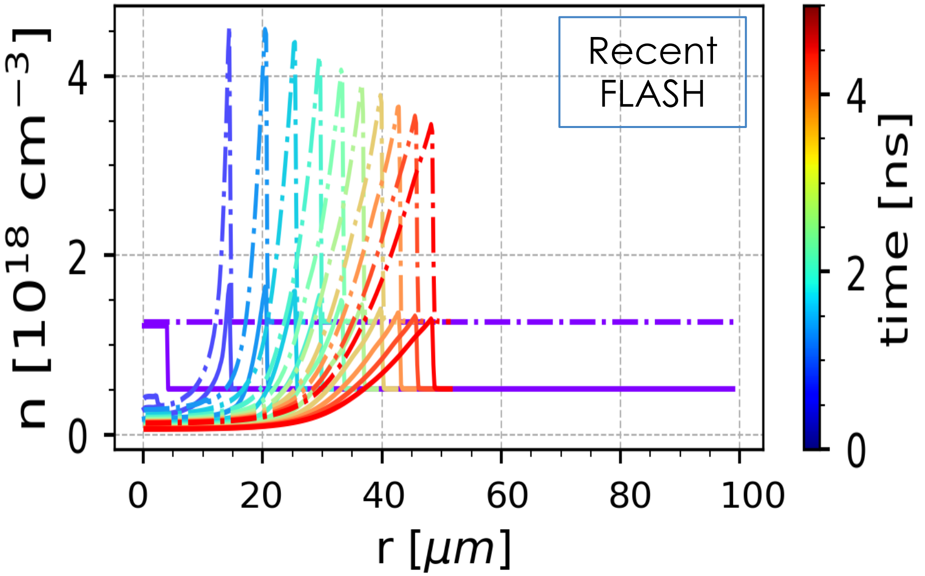

- More work is needed to explore these sensitivities
  - Develop models and/or tables with high fidelity at low temps
  - Continued efforts to couple kinetic and fluid phenomena

A modular Sirepo FLASH interface for simulation design

- Interface enables dynamic templating of FLASH simulations through configuration procedure
  - Problem space should reflect user creation rather than pre-built applications
- A significant departure from existing Sirepo applications
  - Executable must be built for each problem

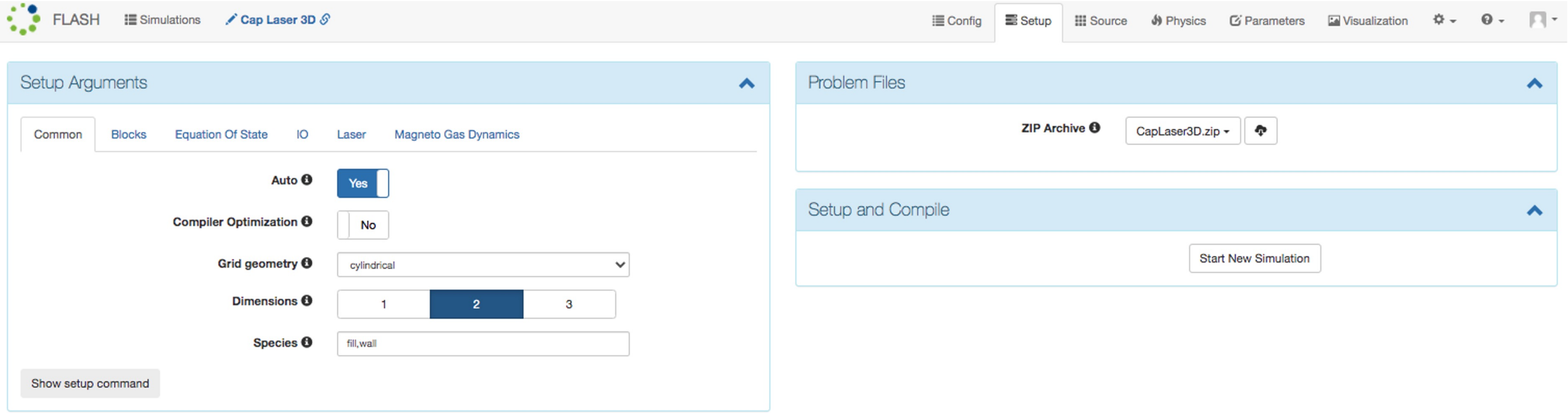

A modular Sirepo FLASH interface for simulation design

- Interface enables dynamic templating of FLASH simulations through configuration procedure
  - Problem space should reflect user creation rather than pre-built applications
- A significant departure from existing Sirepo applications
  - Executable must be built for each problem
  - Accessible units & associated parameters must be updated in conjunction with configuration

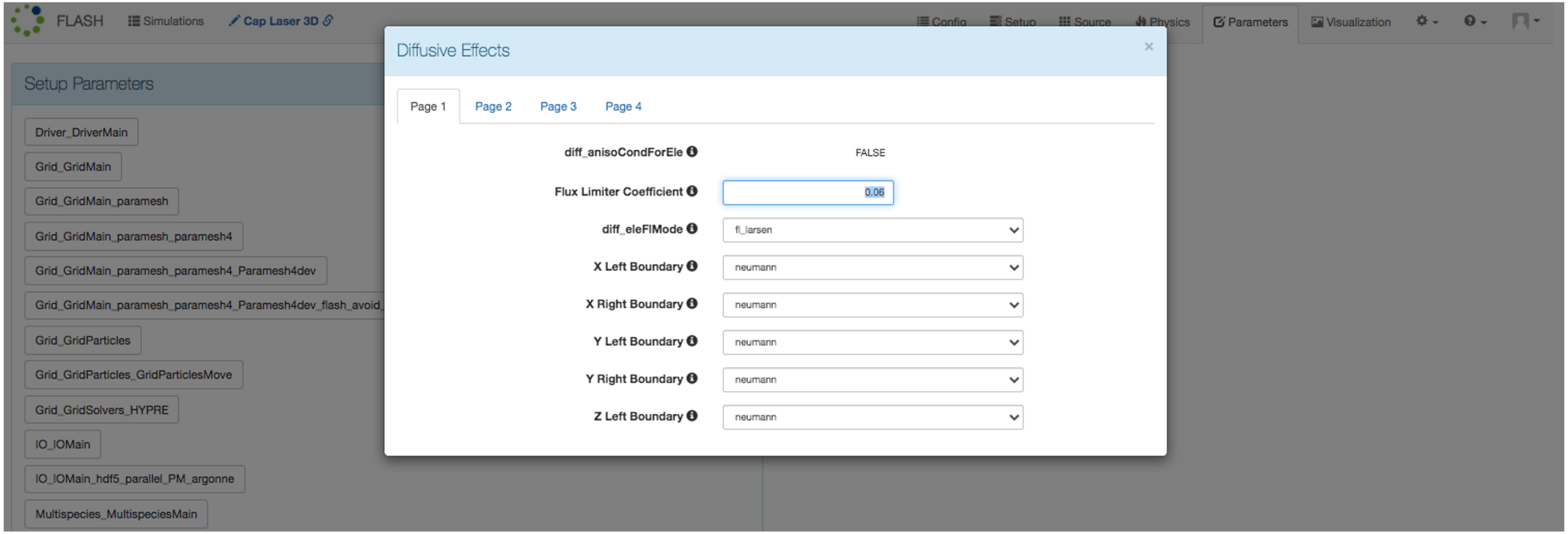

A modular Sirepo FLASH interface for simulation design

- Interface enables dynamic templating of FLASH simulations through configuration procedure
    - Problem space should reflect user creation rather than pre-built applications
- A significant departure from existing Sirepo applications
    - Executable must be built for each problem
    - Accessible units & associated parameters must be updated in conjunction with configuration
    - Analyses must adapt to problem space, variables, and geometry using available metadata

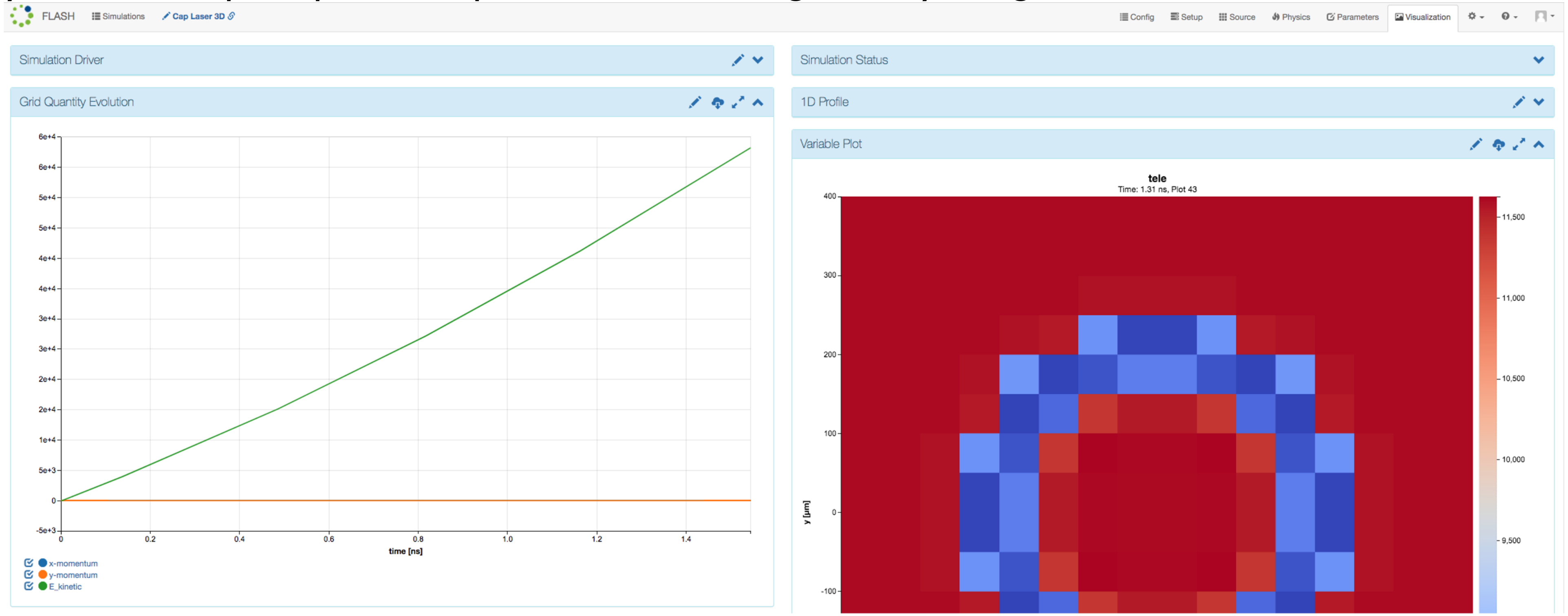

Thanks for your attention!

This material is based upon work supported by the U.S. Department of Energy, Office of Science, Office of High Energy Physics, under Award Number DE-SC0018719

Disclaimer

This report was prepared as an account of work sponsored by an agency of the United States Government. Neither the United States Government nor any agency thereof, nor any of their employees, makes any warranty, express or implied, or assumes any legal liability or responsibility for the accuracy, completeness, or usefulness of any information, apparatus, product, or process disclosed, or represents that its use would not infringe privately owned rights. Reference herein to any specific commercial product, process, or service by trade name, trademark, manufacturer, or otherwise does not necessarily constitute or imply its endorsement, recommendation, or favoring by the United States Government or any agency thereof. The views and opinions of authors expressed herein do not necessarily state or reflect those of the United States Government or any agency thereof.